Results

BCL11B expression

We obtained *Bcl11b*$^{-/-}$ and *Bcl11b*$^{+/+}$ newborn mice by crossing *Bcl11b*$^{+/-}$ heterozygous mice and immunohistochemically examined BCL11B expression in cells of the cochlea (Fig. 1A). The organ of Corti resides on the basilar membrane and typically comprises one row of inner hair cells and three rows of outer hair cells interdigitated with several types of morphologically distinct non-sensory supporting cells. Analysis of *Bcl11b*$^{+/+}$ mice revealed BCL11B expression in the outer hair cells but not in the inner hair cells. No expression was detected in other cell types in the cochlea including spiral ganglion cells. In contrast, *Bcl11b*$^{-/-}$mice did not show BCL11B expression in the outer hair cells. Despite *Bcl11b*$^{-/-}$ mice lacking the BCL11B expression, they did not show any marked change in the morphology of the cochlea. One exception to this was the impaired formation of stereocilia at the top of outer, but not inner, hair cells in *Bcl11b*$^{-/-}$ mice, as revealed by scanning electron microscopy (Fig. 1B).

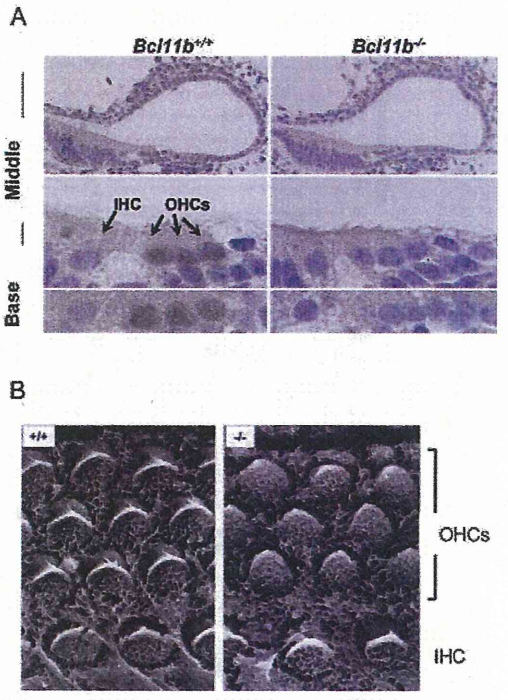

Fig. 1. BCL11B expression and hair cell morphology in *Bcl11b*$^{-/-}$ and *Bcl11b*$^{+/+}$ newborn mice. (A) Immunohistochemistry of BCL11B in the cochlea. The positions of outer (OHC) and inner (IHC) hair cells are marked. (B) Scanning electron microscopy of outer and inner hair cells in the middle turn of the cochlea.

Hearing function in heterozygous Bcl11b$^{+/-}$ *mice*

Outer hair cells are assumed to be the mechanical amplifiers for sound sensitivity and frequency selectivity, and inner hair cells are assumed to be passive detectors of the amplified vibratory signal [5]. We thus tested whether or not heterozygous deletion of *Bcl11b* affects hearing function by analyzing ABR, which is the evoked potential response of auditory activity in the auditory nerve and subsequent fiber tracts and nuclei within the auditory brainstem pathways. Thresholds and amplitudes of ABRs provide information on the peripheral hearing status and the integrity of brainstem pathways [13]. ABRs to frequency-specific stimulation (f-ABR) were measured in *Bcl11b*$^{+/-}$ and *Bcl11b*$^{+/+}$ mice (n=11) of B6 background over various frequency ranges at different months of age (Fig. 2A). Almost all wild-type B6 mice retained low ABR thresholds until 4 months of age; however, mice at 5 or 6 months of age showed some threshold elevations, consistent with previous studies [14, 32]. This progressive AHL in B6 mice is mainly due to their bearing the *Cdh23*^{ahl} and *Ahl3* susceptible alleles on the chromosomes 10 and 17, respectively [14, 22, 23]. Most *Bcl11b*$^{+/-}$ mice showed significant increases in ABR thresholds relative to *Bcl11b*$^{+/+}$ mice at all ages though some still retained low thresholds. The average increases were 10–30 dB SPL at various frequencies ranging from 8 to 32 kHz (Fig. 2A). The hearing loss was detected in mice as early as 3 months of age at 16 and 20 kHz (P=0.038 and P=0.004, respectively). Another independent experiment showed similar results (data not shown).

We also examined BALB/c mice (n=5) that are classified as a normal hearing strain for AHL, despite carrying the *Cdh23*^{ahl} susceptible allele [23]. Figure 2B shows ABR thresholds at various frequency ranges in 9-month old mice. Low ABR thresholds were retained in *Bcl11b*$^{+/+}$ mice whereas a small increase of the ABR threshold was observed in *Bcl11b*$^{+/-}$ mice at 20 kHz but it was not marked at the other frequencies examined. This suggests that the effect of *Bcl11b* heterozygous deletion is small in BALB/c mice.

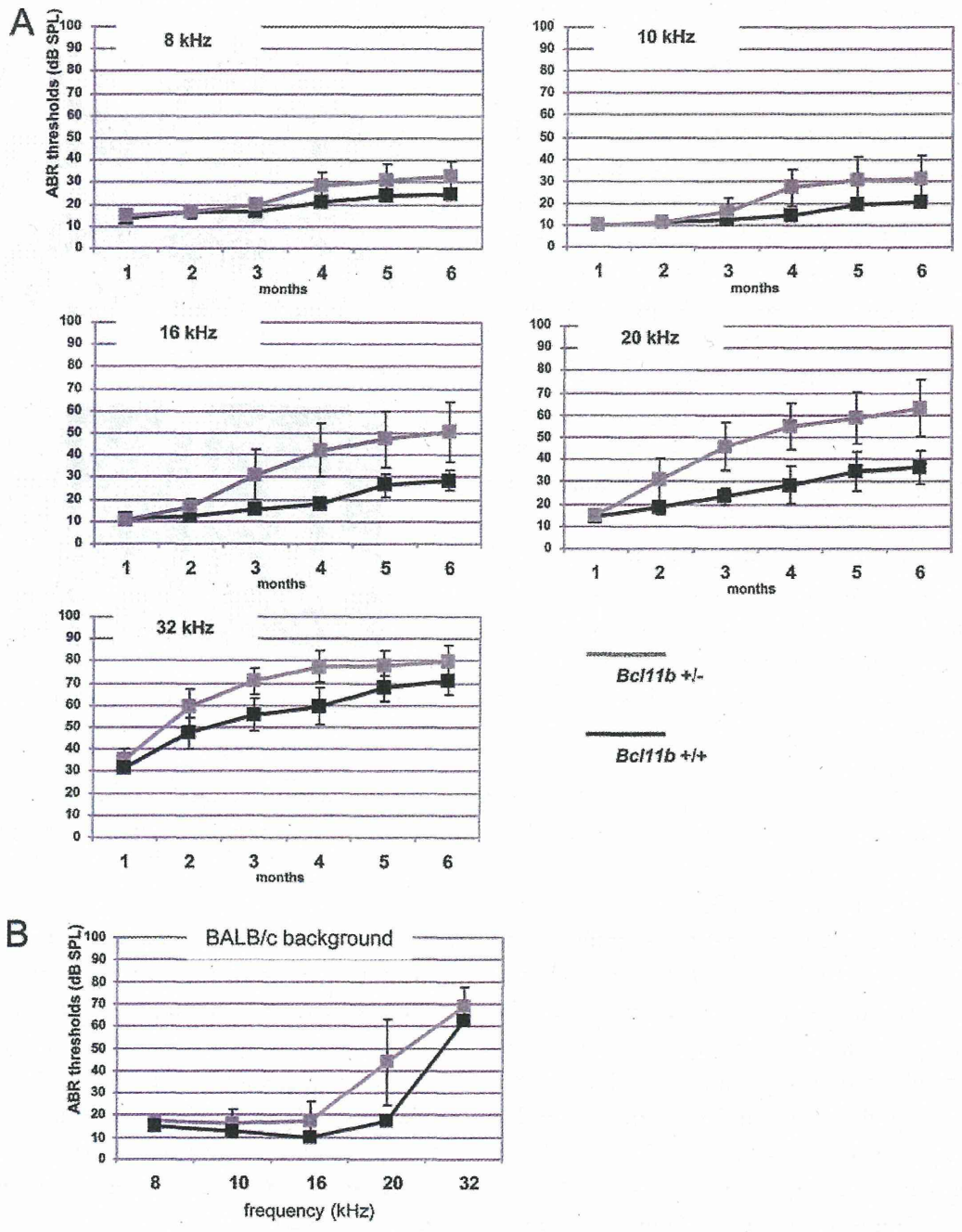

Fig. 2. ABR thresholds of mice of *Bcl11b*$^{+/-}$ and *Bcl11b*$^{+/+}$ genotypes. (A) Data at various frequencies ranging from 8 to 32 kHz are separately shown for C57BL/6 mice at the indicated months of age. (B) Data for BALB/c mice at 9 months of age are shown at different frequency ranges.

Inner ear pathology in heterozygous Bcl11b$^{+/-}$ *mice*

To address whether or not the observed hearing loss in *Bcl11b*$^{+/-}$ mice was accompanied by morphological alterations, we examined the hair cells of the cochlea in 6-month old *Bcl11b*$^{+/-}$ mice with AHL by scanning electron microscopy. Loss of outer hair cells in the cochlea and impairment of stereocilia were evident in some of the mice (Fig. 3A). Such abnormalities were not detected in *Bcl11b*$^{+/+}$ mice. The number of spiral ganglion cells in the cochlea of *Bcl11b*$^{+/-}$ mice seemed to differ

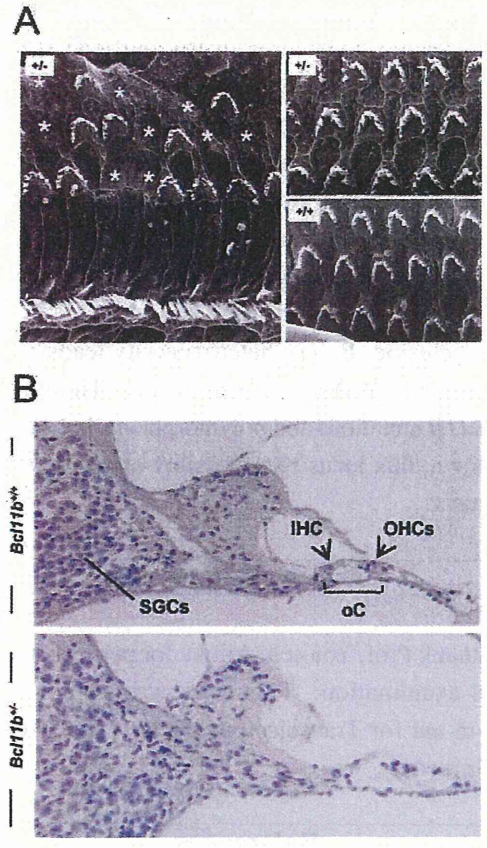

Fig. 3. The morphology of the middle turn of the cochlea in *Bcl11b*$^{+/-}$ mice and *Bcl11b*$^{+/+}$ mice. (A) Scanning electron microscopy of hair cells in the 6-month old *Bcl11b*$^{+/-}$ mice with hearing loss and control *Bcl11b*$^{+/+}$ mice. Loss of hair cells (indicated by *) and impairment of stereocilia are seen in the left panel, and only impairment of stereocilia in the right upper panel. There are no marked changes in the right lower panel. (B) Hematoxylin staining of spiral ganglia (SGC).

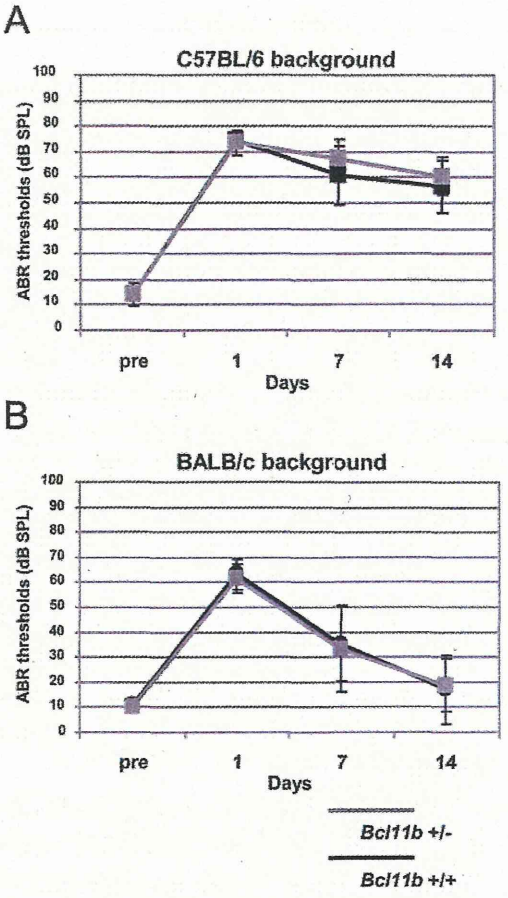

Fig. 4. ABR thresholds in mice at the indicated days after noise exposure at 100 dB SPL for 60 min. (A) C57BL/6 mice of *Bcl11b*$^{+/-}$ and *Bcl11b*$^{+/+}$ genotypes. (B) BALB/c mice of *Bcl11b*$^{+/-}$ and *Bcl11b*$^{+/+}$ genotypes.

from those of their wild-type littermates though the difference was not marked (Fig. 3B). Minimal differences were also observed in the stria vascularis of the cochlea (data not shown).

No difference in hearing loss after acoustic trauma

Our previous study showed that the inhibition of BCL11B in Jurkat cells and thymocytes *in vitro* increased apoptosis sensitivity to stimulation of cell proliferation by increasing the serum concentration and DNA damage by UV irradiation [16]. This suggests that BCL11B activity may be required for cell survival under pathological conditions. We thus examined changes in the ABR thresholds of 2-month-old B6 and BALB/c mice after noise exposure at 100 dB SPL for 60 min. Both strains exhibited significant threshold increases to 50–60 dB SPL one day after noise exposure (Fig. 4). In B6 mice this threshold shift was mostly retained at 7 and 14 days after noise exposure, and the shifts on different days did not differ between *Bcl11b*$^{+/-}$ and *Bcl11b*$^{+/+}$ mice (Fig. 4A). Also, no difference between the *Bcl11b*$^{+/-}$ and *Bcl11b*$^{+/+}$ genotypes was observed in the threshold shift in BALB/c mice, though both had restored low ABR thresholds at 14 days after noise exposure (Fig. 4B). These results suggest that the heterozygous deletion of *Bcl11b* does not affect cochlear vulnerability to noise-induced hearing loss.

Discussion

The results of this study show that BCL11B transcription factor is expressed in the cell nucleus of outer hair cells, but not inner hair cells, of the mouse cochlea and that the heterozygous deletion of *Bcl11b* leads to a progressive age-related hearing loss, which was evident in mice as young as 3 months of age. Loss of outer hair cells was observed in the $Bcl11b^{+/-}$ mice with hearing loss at 6 months after birth. These results suggest that the AHL observed in $Bcl11b^{+/-}$ mice is the result of impairment of the outer hair cells, classified as the sensory type of presbycusis, and that BCL11B activity is required for the maintenance of outer hair cells and normal hearing. However, many questions remain. For instance, how does BCL11B protect outer hair cells and hearing function against aging? A target of BCL11B transcription factor is *p27* [16] and $p27^{-/-}$ mice exhibit hearing loss [17]. However, p27 was not expressed in the outer hair cells though it was expressed in nearby supporting cells (data not shown).

The effect of the *Bcl11b* heterozygous deletion on AHL was less in BALB/c mice than B6 mice, reflecting their different genetic backgrounds. This suggests the involvement of one or more genetic loci responsible for AHL susceptibility other than the *Bcl11b* locus, though the relevant genetic difference between the two mouse strains is unknown. B6 mice carry at least two alleles ($Cdh23^{ahl}$ and *Ahl3*) that promote AHL and sensory hair cell loss whereas BALB/c mice are only known to carry the $Cdh23^{ahl}$ allele [14, 22, 23]. *Cdh23* encodes cadherin 23, a component of the tip links joining adjacent stereocilia at the top of sensory outer and inner hair cells [25, 26]. Its null mutation causes congenital deafness in mice and humans accompanying degeneration of the stereocilia of outer and inner hair cells [2, 3, 7, 30]. *Bcl11b* and *Cdh23* are both expressed in outer hair cells and affect AHL but their relationship with the development of AHL is unclear.

Mechanical stress is a factor affecting AHL, and genetic variation affects the range of individual susceptibility to mechanically induced acoustic trauma [6]. In fact, the $Cdh23^{ahl}$ susceptible allele renders mice more susceptible to noise-induced hearing loss than strains that do not carry this allele [8, 29]. We tested the effect of *Bcl11b* heterozygosity on cochlear vulnerability to acoustic energy exposures in B6 and BALB/c mice. However, no difference was detected between $Bcl11b^{+/+}$ and $Bcl11b^{+/-}$ genotypes in either mouse strain. This suggests that *Bcl11b* heterozygous deletion or probably the AHL-susceptible $Bcl11b^{+/-}$ outer hair cells do not contribute to the vulnerability to acoustic energy exposures. Hence, involvement of *Cdh23* and *Bcl11b* is different in noise-induced hearing loss.

In conclusion, *Bcl11b* heterozygosity leads to a progressive age-related hearing loss in mice. Though details of *BCL11B* mutations and polymorphisms in humans are not known, this locus may possibly affect presbycusis in humans.

Acknowledgments

We thank Prof. You-ichi Ajioka for performing histological examination. This work was supported by a Grant-in-aid for Transdisciplinary Research from Niigata University.

References

1. Arlotta, P., Molyneaux, B.J., Chen, J., Inoue, J., Kominami, R., and Macklis, J.D. 2005. Neuronal subtype-specific genes that control corticospinal motor neuron development in vivo. *Neuron* 45: 207–221.
2. Astuto, L.M., Bork, J.M., Weston, M.D., Askew, J.W., Fields, R.R., Orten, D.J., Ohliger, S.J., Riazuddin, S., Morell, R.J., Khan, S., Riazuddin, S., Kremer, H., van Hauwe, P., Moller, C.G., Cremers, C.W., Ayuso, C., Heckenlively, J.R., Rohrschneider, K., Spandau, U., Greenberg, J., Ramesar, R., Reardon, W., Bitoun, P., Millan, J., Legge, R., Friedman, T.B., and Kimberling, W.J. 2002. CDH23 mutation and phenotype heterogeneity: a profile of 107 diverse families with Usher syndrome and nonsyndromic deafness. *Am. J. Hum. Genet.* 71: 262–275.
3. Bolz, H., von Brederlow, B., Ramirez, A., Bryda, E.C., Kutsche, K., Nothwang, H.G., Seeliger, M., del C-Salcedo, M., Cabrera, M., Vila, M.C., Molina, O.P., Gal, A., and Kubisch, C. 2001. Mutation of CDH23, encoding a new member of the cadherin gene family, causes Usher syndrome type 1D. *Nat. Genet.* 27: 108–112.
4. Cherrier, T., Suzanne, S., Redel, L., Calao, M., Marban, C., Samah, B., Mukerjee, R., Schwartz, C., Gras, G., Sawaya, BE., Zeichner, SL., Aunis, D., Van Lint, C., and Rohr, O. 2009. p21(WAF1) gene promoter is epigenetically silenced by CTIP2 and SUV39H1. *Oncogene* 28: 3380–3389.
5. Dallos, P., Wu, X., Cheatham, M.A., Gao, J., Zheng, J., Anderson, C.T., Jia, S., Wang, X, Cheng, W.H., Sengupta,

S., He, D.Z., and Zuo, J. 2008. Prestin-based outer hair cell motility is necessary for mammalian cochlear amplification, *Neuron* 58: 333–339.

6. Davis, R.R., Newlander, J.K., Ling, X., Cortopassi, G.A., Krieg, E.F., and Erway, L.C. 2001. Genetic basis for susceptibility to noise-induced hearing loss in mice. *Hear. Res.* 155: 82–90.
7. Di Palma, F., Holme, R.H., Bryda, E.C., Belyantseva, I.A., Pellegrino, R., Kachar, B., Steel, K.P., and Noben-Trauth, K. 2001. Mutations in Cdh23, encoding a new type of cadherin, cause stereocilia disorganization in waltzer, the mouse model for Usher syndrome type 1D. *Nat. Genet.* 27: 103–107.
8. Erway, L.C., Shiau, Y.W., Davis, R.R., and Krieg, E.F. 1996. Genetics of agerelated hearing loss in mice. III. Susceptibility of inbred and F1 hybrid strains to noise-induced hearing loss. *Hear. Res.* 93: 181–187.
9. Golonzhka, O., Liang, X., Messaddeq, N., Bornet, J.M., Campbell, A.L., Mertzger, D., Chambon, P., Ganguli-Indra, G., Leid, M., and Indra, A. 2009. Dual role of COUP-TF-interacting protein 2 in epidermal homeostasis and permeability barrier formation. *J. Invest. Dermatol.* 129: 1459–1470.
10. Golonzhka, O., Metzger, D., Bornert, J.M., Bay, B.K., Gross, M.K., Kioussi, C., and Leid, M. 2009. Ctip2/Bcl11b controls ameloblast formation during mammalian odontogenesis. *Proc. Natl. Acad. Sci. U.S.A.* 106: 4278–4283.
11. Gorlin, R.J., Toriello, H.V., and Cohen, M.M. 1995. Hereditary Hearing Loss and Its Syndromes, Oxford University Press, New York, Oxford.
12. Grabarczyk, P., Przybylski, G.K., Depke, M., Volker, U., Bahr, J., Assmus, K., Broker, B.M., Walther, R., and Schmidt, C.A. 2007. Inhibition of BCL11B expression leads to apoptosis of malignant but not normal mature T cells. *Oncogene* 26: 3797–3810.
13. Jewett, D.L., Romano, M.N., and Williston, J.S. 1970. Human auditory evoked potentials: possible brain stem components detected on the scalp. *Science* 167: 1517–1518.
14. Johnson, K.R., Erway, L.C., Cook, S.A., Willott, J.F., and Zheng, Q.Y. 1997. A major gene affecting age-related hearing loss in C57BL/6J mice. *Hear. Res.* 114: 83–92.
15. Kamimura, K., Ohi, H., Kubota, T., Okazuka, K., Yoshikai, Y., Wakabayashi, Y., Aoyagi, Y., Mishima, Y., and Kominami, R. 2007. Haploinsufficiency of Bcl11b for suppression of lymphomagenesis and thymocyte development. *Biochem. Biophys. Res. Commun.* 355: 538–542.
16. Kamimura, K., Mishima, Y., Obata, M., Endo, T., Aoyagi, Y., and Kominami, R. 2007. Lack of Bcl11b tumor suppressor results in vulnerability to DNA replication stress and damages. *Oncogene* 26: 5840–5850.
17. Kanzaki, S., Beyer, L.A., Swiderski, D.L., Izumikawa, M., Stöver, T., Kawamoto, K., and Raphael, Y. 2006. $p27^{Kip1}$ deficiency causes organ of Corti pathology and hearing loss. *Hear. Res.* 214: 28–36.
18. Li, H.S. and Hultcrantz, M. 1994. Age-related degeneration of the organ of Corti in two genotypes of mice. *ORL J. Otorhinolaryngol. Relat. Spec.* 56: 61–67.
19. Morita, Y., Hirokawa, S., Kikkawa, Y., Nomura, T., Yonekawa, H., Shiroishi, T., Takahashi, S., and Kominami, R. 2007. Fine mapping of Ahl3 affecting both age-related and noise-induced hearing loss. *Biochem. Biophys. Res. Commun.* 355: 117–121.
20. Morton, N.E. 1991, Genetic epidemiology of hearing loss. *Ann. N.Y. Acad. Sci.* 630: 16–31.
21. Mulrow, C.D. 1990. Association between hearing impairment and the quality of life of elderly individuals. *J. Am. Geriatr. Soc.* 38: 45–50.
22. Nemoto, M., Morita, Y., Mishima, Y., Takahashi, S., Nomura, T., Ushiki, T., Shiroishi, T., Kikkawa, Y., Yonekawa, H., and Kominami, R. 2004. Ahl3, a third locus on mouse chromosome 17 affecting age-related hearing loss. *Biochem. Biophys. Res. Commun.* 324: 1283–1288.
23. Noben-Trauth, K., Zheng, Q.Y., and Johnson, K.R. 2003. Association of cadherin 23 with polygenic inheritance and genetic modification of sensorineural hearing loss. *Nat. Genet.* 35: 21–23.
24. Ohlemiller, K.K. 2006. Contributions of mouse models to understanding of age- and noise-related hearing loss. *Brain Res.* 26: 89–102.
25. Siemens, J., Lillo, C., Dumont, R.A., Reymonds, A., Williams, D.S., Gillespie, P.G., and Muller, U. 2004. Cadherin 23 is a component of the tip link in hair-cell stereocillia. *Nature* 428: 950–955.
26. Sollner, C., Rauch, G.J., Siemens, J., Geisler, R., Schuster, S.C., Muller, U., and Nicolson, T. 2004. Mutations in cadherin 23 affect tip links in zebrafish sensory hair cells. *Nature* 428: 955–959.
27. Spongr, V.P., Flood, D.G., Frisina, R.D., and Salvi, R.J. 1997. Quantitative measures of hair cell loss in CBA and C57BL/6 mice throughout their life spans. *J. Acoust. Soc. Am.* 101: 3546–3553.
28. Topark-Ngarm, A., Golonzhka, O., Peterson, V.J., Barrett, B. Jr., Martinez, B., Crofoot, K., Filtz, T.M., and Leid, M. 2006. CTIP2 associates with the NuRD complex on the promoter of p57KIP2, a newly identified CTIP2 target gene. *J. Biol. Chem.* 281: 32272–32283.
29. Vazquez, A.E., Jimenez, A.M., Martin, G.K., Luebke, A.E., and Lonsbury-Martin, B.L. 2004. Evaluating cochlear function and the effects of noise exposure in the B6. CAST+Ahl mouse with distortion product otoacoustic emissions. *Hear. Res.* 194: 87–96.
30. Wada, T., Wakabayashi, Y., Takahashi, S., Ushiki, T., Kikkawa, Y., Yonekawa, H., and Kominami, R. 2001. A point mutation in a cadherin gene, Cdh23, causes deafness in a novel mutant, Waltzer mouse niigata. *Biochem. Biophys. Res. Commun.* 283: 113–117.
31. Wakabayashi, Y., Watanabe, H., Inoue, J., Takeda, N., Sakata, J., Mishima, Y., Hitomi, J., Yamamoto, T., Utsuyama, M., Niwa, O., Aizawa, S., and Kominami, R. 2003. Bcl11b is required for differentiation and survival of T lymphocytes. *Nat. Immunol.* 5: 533–539.
32. Zheng, Q.Y., Johnson, K.R., and Erway, L.C. 1999. Assessment of hearing in 80 inbred strains of mice by ABR threshold analyses. *Hear. Res.* 130: 94–107.

Int. J. Radiation Oncology Biol. Phys., Vol. 77, No. 1, pp. 235–243, 2010

0360-3016/10/$–see front matter

ELSEVIER

doi:10.1016/j.ijrobp.2009.11.005

BIOLOGY CONTRIBUTION

CLONALLY EXPANDING THYMOCYTES HAVING LINEAGE CAPABILITY IN GAMMA-RAY–INDUCED MOUSE ATROPHIC THYMUS

TAKASHI YAMAMOTO, M.D.,*† SHIN-ICHI MORITA, M.D.,*† RIEKA GO, D.D.S.,* MIKI OBATA, B.SCI.,* YOSHINORI KATSURAGI, PH.D.,* YUKARI FUJITA, M.SCI.,* YOSHITAKA MAEDA, B.SCI.,‡ MINESUKE YOKOYAMA, PH.D.,‡ YUTAKA AOYAGI, M.D., PH.D.,† HITOSHI ICHIKAWA, PH.D.,§ YUKIO MISHIMA, PH.D.,* AND RYO KOMINAMI, M.D., PH.D.*

*Department of Molecular Genetics and †3rd Internal Medicine, Niigata University Graduate School of Medical and Dental Sciences, Niigata, Japan; ‡Center for Bioresource-Based Researches, Brain Research Institute, Niigata, Japan; and §Genetics Division, National Cancer Center Research Institute, Tokyo, Japan

Purpose: To characterize, in the setting of γ-ray–induced atrophic thymus, probable prelymphoma cells showing clonal growth and changes in signaling, including DNA damage checkpoint.
Methods and Materials: A total of 111 and 45 mouse atrophic thymuses at 40 and 80 days, respectively, after γ-irradiation were analyzed with polymerase chain reaction for D-J rearrangements at the *TCRβ* locus, flow cytometry for cell cycle, and Western blotting for the activation of DNA damage checkpoints.
Results: Limited D-J rearrangement patterns distinct from normal thymus were detected at high frequencies (43 of 111 for 40-day thymus and 21 of 45 for 80-day thymus). Those clonally expanded thymocytes mostly consisted of $CD4^+CD8^+$ double-positive cells, indicating the retention of lineage capability. They exhibited pausing at a late G1 phase of cell cycle progression but did not show the activation of DNA damage checkpoints such as γH2AX, Chk1/2, or p53. Of interest is that 17 of the 52 thymuses showing normal D-J rearrangement patterns at 40 days after irradiation showed allelic loss at the *Bcl11b* tumor suppressor locus, also indicating clonal expansion.
Conclusion: The thymocytes of clonal growth detected resemble human chronic myeloid leukemia in possessing self-renewal and lineage capability, and therefore they can be a candidate of the lymphoma-initiating cells. © 2010 Elsevier Inc.

Gamma-ray–induced mouse thymic lymphoma, Prelymphoma, DNA damage response, Bcl11b, Cancer stem cells.

INTRODUCTION

Premalignant conditions are recognizable lesions that are strongly associated with the development of malignant neoplasia. One such lesion must exist in γ-ray–induced mouse atrophic thymus because mice that received thymocytes from the atrophic thymus developed thymic lymphomas at a high frequency (1, 2). Immature thymocytes in the thymus proliferate and undergo β-selection at $CD4^-$ and $CD8^-$ double-negative stage and differentiate into double-positive (DP) cells, which further differentiate into $CD4^+$ or $CD8^+$ single-positive cells (3, 4). The thymus controls the cellular fate of thymocytes, including the elimination of unfavorable cells that are generated during developmental and pathologic processes (5).

Chronic myeloid leukemia (CML) may have a characteristic of the premalignant condition because CML cells differentiate to mature, nontumorigenic blood cells though possessing intrinsic self-renewal capability (6, 7). The transition from the CML chronic phase to the aggressive blast crisis phase requires the arrest of differentiation. Because CML arises from hematopoietic stem cell–like progenitors, it is thought to conform well to the cancer stem cell model (8). As described above, because of the tumorigenic capability of thymocytes in the atrophic thymus, thymocytes might contain cancer stem cells or lymphoma-initiating cells. The importance of leukemia-initiating cells is pointed out in relapsed acute lymphoblastic leukemia in humans, in that the cells responsible for relapse are ancestral to the primary leukemia cells (9).

Normal cells can perceive and arrest aberrant cycles of cell division that are triggered by cancer-promoting stimuli. A hallmark of precancerous cells in major human cancer types is aberrant stimulation of cell proliferation that results in

Reprint requests: Ryo Kominami, M.D., Department of Molecular Genetics, Niigata University Graduate School of Medical and Dental Sciences, Asahimachi 1-757, Chuo-ku, Niigata 951-8510, Japan. Tel: (+81) 25-227-2077; Fax: (+81) 25-227-0757; E-mail: rykomina@med.niigata-u.ac.jp

T.Y. and S.M. contributed equally to this work.

This work was supported by grants-in-aid for Cancer Research from the Ministries of Education, Science, Art and Sports, and Health and Welfare of Japan.

Conflict of interest: none.

Received Aug 20, 2009, and in revised form Nov 5, 2009. Accepted for publication Nov 7, 2009.

DNA replication stress and the subsequent activation of DNA damage checkpoint (10, 11). The checkpoint functions as an inducible barrier against genomic instability and tumor development (12, 13). The probable prelymphoma cells may exhibit the activation of DNA damage checkpoint, or they may show difference in oncogenic signals because lymphomas/leukemias are distinct in origin from carcinomas. Indeed, some disagreement has been reported in the study of T cell lymphomas developed in *PTEN*-deficient mice (14). In this study, we have characterized the probable prelymphoma cells showing clonal growth and changes in signaling, including DNA damage checkpoint.

METHODS AND MATERIALS

Mice and induction of atrophic thymus and lymphoma development

BALB/cAJcl mice (purchased from CLEA Japan, Tokyo, Japan) were mated with MSM mice (provided from Dr. Shiroishi, National Institute of Genetics at Mishima), and their male and female progeny were subjected to whole-body γ-irradiation of 2.5 Gy (^{137}Cs) four times at a weekly interval, starting at the age of 4 weeks. Thymus was isolated at 40 days and 80 days after the start of irradiation. Isolation of thymic lymphomas and bone marrow cell transfer were carried out as described previously (15, 16). Mice used in this study were maintained under specific pathogen-free conditions in the animal colony of Niigata University. All animal experiments comply with the guidelines of the animal ethics committee for animal experimentation of the University.

Flow cytometry

Flow cytometric analysis and 5-bromo-2-deoxyuridine (BrdU) incorporation experiments were performed as previously described (17). The monoclonal antibodies used were anti-CD4-FITC or -APC (RM4-5), anti-CD8-APC (53-6.7), purchased from eBioscience (San Diego, CA). Anti-Nrp-1 (sc-5541; Santa Cruz Biotechnology, Santa Cruz, CA) was detected with anti-rabbit IgG-Alexa Fluor 488 (A11008; Molecular Probes, Invitrogen, Carlsbad, CA.). Dead cells and debris were excluded from the analysis by appropriate gating of forward scatter (FSC) and side scatter (SSC). Cells were analyzed by a FACScan (Becton-Dickinson, Franklin Lakes, NJ) flow cytometer, and data were analyzed using Flow-Jo software (Tree-Star, Ashland, OR).

DNA isolation and PCR analysis

Deoxyribonucleic acid was isolated from brain, thymocytes, and thymic lymphomas using the DNeasy Tissue Kit (Qiagen, Valencia, CA). To determine D-J rearrangement patterns in the *TCRβ* locus, polymerase chain reaction (PCR) was performed as described previously (16). For allelic loss analysis at *Bcl11b*, *D12Mit53* and *D12Mit279* markers were used for PCR as described previously (15). The PCR products were analyzed by 8% polyacrylamide gel electrophoresis, and band intensities were quantitated with a Molecular Imager FX (Bio-Rad Laboratories, Hercules, CA) after ethidium bromide staining to determine the allele ratio of BALB/c and MSM alleles.

Antibodies for Western blotting

Sample preparation and Western blotting were performed as described previously (18). Antibodies used are listed below. Anti-H2AX (ab11175) and anti-Chk2 (pT68) (ab38461) were purchased from Abcam (Cambridge, MA). Anti-p27 Kip1 (#2552), anti-Chk2 (#2662), anti-p53 (pSer15) (#9284), anti-Akt (#9272), and anti-Akt (pSer473) (#4058) were purchased from Cell Signaling Technology (Danvers, MA). Anti-cMyc (sc-42), anti–proliferating cell nuclear antigen (PCNA) (sc-7907), anti-actin (sc-1615), anti-p53 (sc-1312), anti-Chk1 (sc7898), and horseradish peroxidase (HRP)-anti-goat IgG (sc-2020) were purchased from Santa Cruz Biotechnology. Anti-cyclin D1 (K0062-3) was purchased from MBL (Nagoya, Japan). Anti-Chk1(pS317) (AF473) was purchased from R&D Systems (Minneapolis, MN). Horseradish peroxidase-anti-rabbit IgG (NA934 V) and HRP-anti-mouse IgG (NA931VS) were purchased from Amersham (Piscataway, NJ). Anti-γH2AX (Ser139) (#07-164) was purchased from Upstate (Temecula, CA).

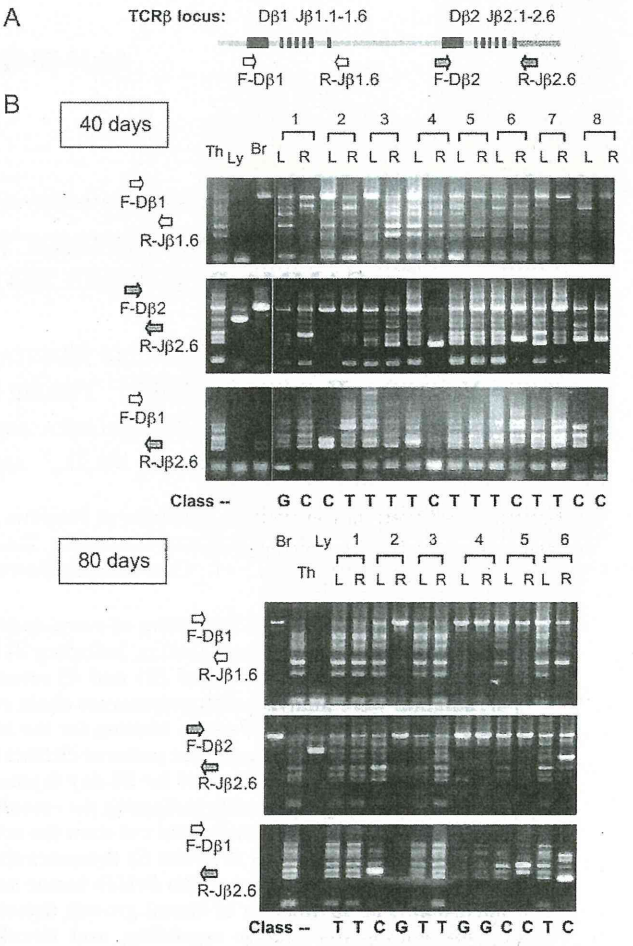

Fig. 1. Clonal growth of thymocytes in atrophic thymuses at 40 days and 80 days after γ-irradiation. (A) Diagram showing part of the *TCRβ* locus and the relative location of polymerase chain reaction (PCR) primers used. (B) Gel electrophoresis of PCR products with three different sets of primers: F-Dβ1 and R-Jβ1.6 (top), F-Dβ2 and to-Jβ2.6 (middle), and F-Dβ1 and R-Jβ2.6 (bottom). Th = thymus; Ly = lymphomas; Br = barain DNA; L and R = left and right thymic lobe; T = T type thymus; C = C type thymus; G = G type thymus.

RESULTS

Clonal expansion of thymocytes in γ-ray–induced atrophic thymus

Clonality of thymocytes was examined in left and right lobes separately of atrophic thymuses at 40 and 80 days after

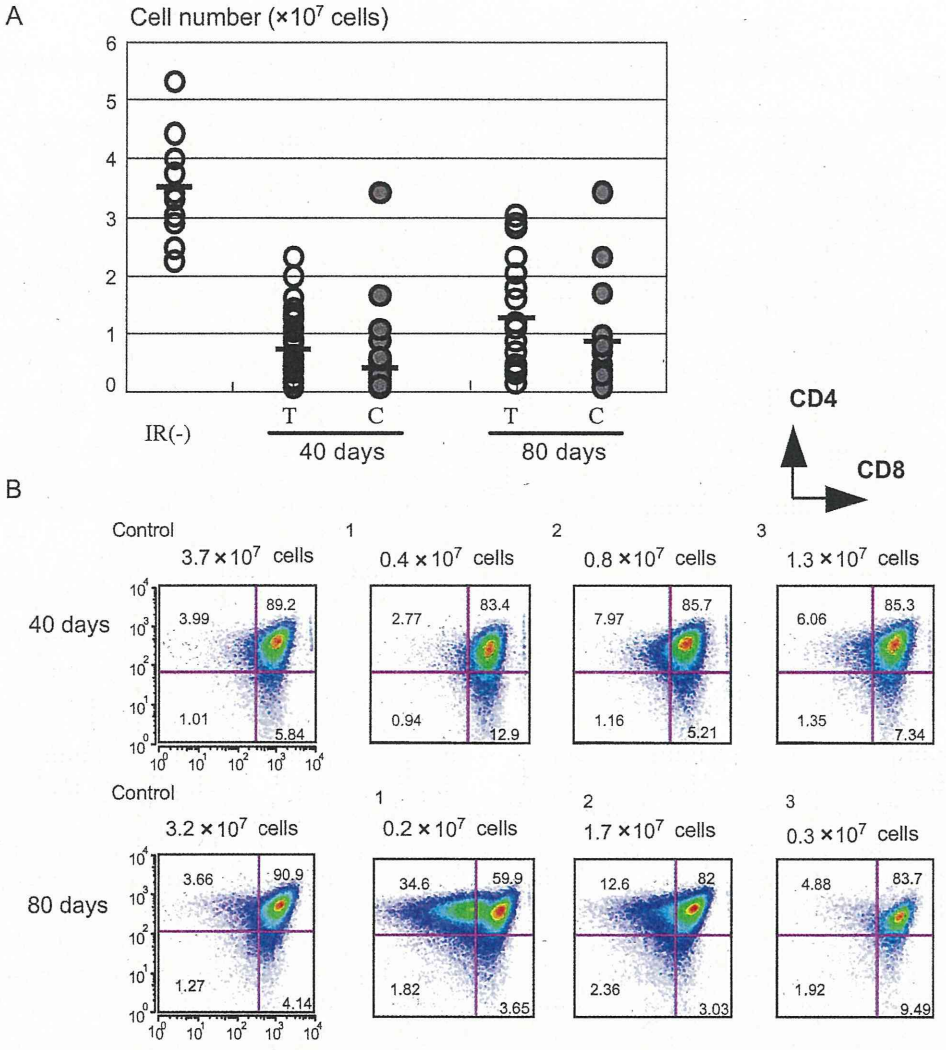

Fig. 2. Reduced cellularity and minimal changes of thymocyte differentiation in atrophic thymuses. (A) Cell numbers of thymocytes in unirradiated thymus and the atrophic thymuses at 40 days and 80 days after irradiation, which were divided into the T type (T) and C type (C) thymus. Bars indicate averages. (B) Flow cytometric analysis of thymocytes from C type thymuses using CD4 and CD8 cell-surface markers. Numbers in quadrants indicate percentage of cells.

γ-irradiation (hereafter these thymic lobes are designated as 40-day and 80-day thymuses, respectively). The earliest time of appearance of fully malignant thymic lymphomas is approximately 100 days after irradiation, and 60% of mice develop lymphomas at 300 days after (5, 16). Clonality was determined in 111 samples of 40-day thymuses and 45 samples of 80-day thymuses by assaying specific V(D)J rearrangements with three primer sets designed for the *TCRβ* locus (16). Figure 1 shows examples, and Supplementary Figs. E1A and B display others. Unirradiated thymus (lane Th) gave six different bands corresponding to possible recombination sites between D and J regions by Dβ1-Jβ1, Dβ2-Jβ2, and Dβ1-Jβ2 probe sets and one band for germline DNA by the former two probe sets. On the other hand, thymic lymphoma DNA (Ly) gave one band only by the Dβ2-Jβ2 probe set used, and brain DNA (Br) gave the germline DNA band by Dβ1-Jβ1 and Dβ2-Jβ2 probe sets. Half (52 of 111) of the 40-day thymuses showed rearrangement patterns identical or similar to that of the control thymus, classified as T type thymus. Most others (43) exhibited only few bands or limited numbers of bands. This group of the thymuses indicated the existence of clonally expanded thymocytes (C type thymus). Several thymuses were classified as C/T type thymus. The fourth group comprised 12 thymuses that exhibited mainly one germline band, probably consisting of immature thymocytes and/or cells other than thymocytes. This study excluded analysis of the G type thymus because of its low incidence. Of the 80-day thymuses, 22 thymuses belonged to T type thymus, and 20 were C type thymus.

Figure 2A shows the thymocyte numbers of 40-day and 80-day thymuses. The average decreased by approximately one seventh in 40-day thymuses, and the decrease tended to be more in C type thymus than in T type thymus. The tendency of decrease was continued in 80-day thymuses. Flow cytometry using CD4 and CD8 cell-surface markers revealed that most thymocytes were DP cells, as normal thymocytes

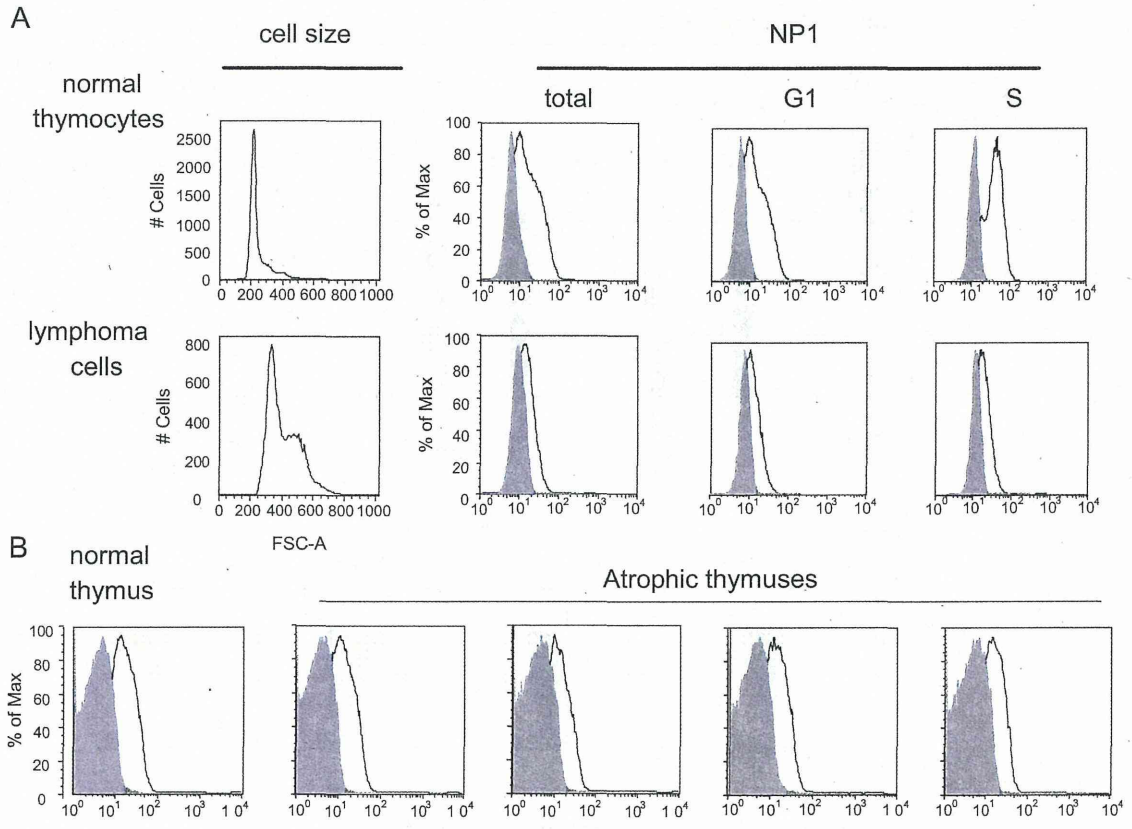

Fig. 3. Flow cytometry of Nrp-1 expression on thymocytes. (A) Profiles of FSC analysis and Nrp-1 staining in total, S phase, and G1 phase cells of unirradiated thymus and thymic lymphoma. Shadowed profiles show control staining without using anti-Nrp-1 antibody. (B) Nrp-1 staining in 40-day atrophic thymuses.

were (Fig. 2B). These findings suggest decrease in the cell number and no marked change in differentiation in atrophic thymus.

Bone marrow cell transfer to irradiated mice 1 week after the last irradiation suppresses the development of thymic lymphomas (1). To confirm this, we examined eight thymic lobes at 60 days after bone marrow cell transfer. As predicted, the cell number was restored to the normal level (3.1×10^7 cells on average), and no C type thymuses were found (not shown).

Nrp-1 expression in atrophic thymuses

Nrp-1 proteins are expressed on the cell surface of both thymocytes and thymic epithelial cells and play a key role in heterocellular adhesions (19, 20). We examined Nrp-1 on thymocytes in normal thymus, thymic lymphomas, and 16 40-day atrophic thymuses using flow cytometry. Levels of Nrp-1 expression on normal thymocytes varied in different phases of the cell cycle, higher in S cells than G1 cells (Fig. 3A). On the other hand, levels on lymphoma cells were lower than those on normal thymocytes and did not much differ between S and G1 cells. Figure 3B shows examples of 40-day atrophic thymuses. Most of them exhibited expression levels similar to that of the control. Neither was any marked difference seen between T type and C type thymus (not shown). These results suggest persistence of the interaction between thymocytes and thymic stroma cells even in atrophic thymuses.

Allelic loss at Bcl11b in C type and T type thymuses

Clonal expansion of thymocytes may result from genetic changes. Hence, we examined allelic loss at *Bcl11b* tumor suppressor gene locus, which was detected at a high frequency in thymic lymphomas (15). *Bcl11b* encodes zinc finger transcription factors involved in the development of $\alpha\beta$ T cells (17). Mice used for this experiment were F_1 hybrids between BALB/c and MSM strains, and hence allelic differences were easily detectable with PCR. Figure 4A shows examples of 40-day thymuses including D-J rearrangement patterns (see Fig. E2A for others). We determined the BALB/c and MSM band ratio in a total of 95 40-day atrophic thymuses and compared the ratios between each atrophic thymus and normal F_1 mouse thymus. When the ratio was >2 or <.50, the thymus was judged as allelic loss-positive (Fig. 4B). The loss was detected in not only C type but also T type thymuses. Nineteen (44%) of the 43 C type thymuses and 17 (33%) of the 52 T type thymuses were allelic loss-positive (Fig. 4C). The high frequency observed in T type thymuses was unexpected. This suggests that clonal expansion of this type proceeds in T type DP thymocytes before β-selection.

Analysis of 80-day thymuses (Fig. E2B) showed that 10 (50%) of the 20 C type thymuses but only 1 (5%) of the 22

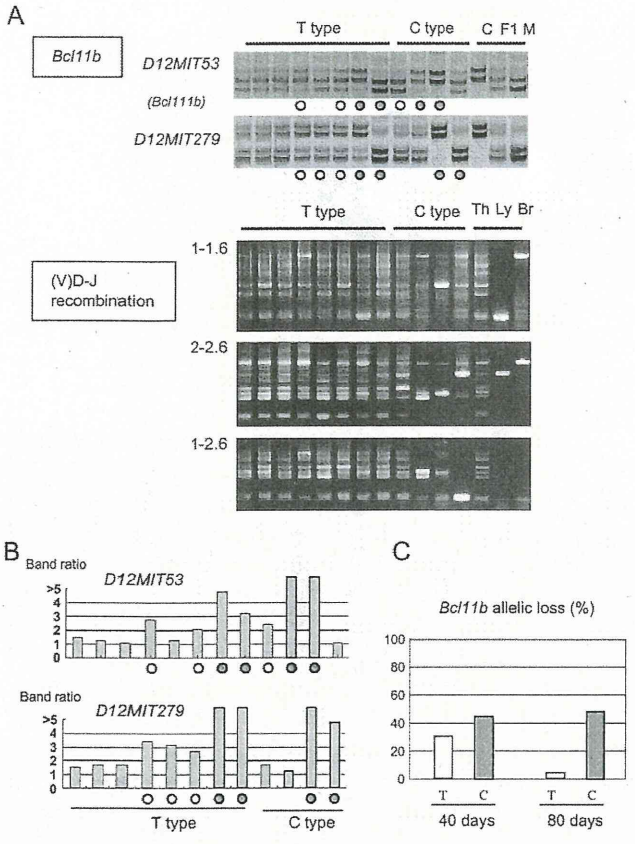

Fig. 4. Allelic losses at the *Bcl11b* locus. (A) Top two panels show polyacrylamide gel electrophoresis for polymerase chain reaction products of *D12Mit53* and *D12Mit279* primer pairs. Chromosomal location of *D12Mit53*, *Bcl11b*, and *D12Mit279* is 108.69 Mb, 109.15–24 Mb, and 109.69 Mb from the centromere, respectively. Bottom three panels show D-J rearrangement patterns, which identifies T type or C type thymus. Closed circles show allelic loss and open circles exhibit allelic imbalance. Thymuses that exhibited allelic loss in at least one of the two loci were decided as allelic loss positive, and this decision was based on three independent polymerase chain reaction experiments. Th = thymus; Ly = lymphomas. (B) Band ratios of BALB/c vs MSM or MSM vs BALB/c are shown relative to that of normal F_1 mouse thymus. Allelic losses are marked by filled circles and allelic imbalances by open circles. (C) Percentage of allelic loss in 40-day and 80-day thymuses that were divided into T type and C type thymus.

T type thymuses exhibited allelic loss. One reason for this rareness relative to 40-day T type thymuses ($p < 0.001$) might be that those T type thymocytes undergo normal differentiation process and hence are not retained within the thymus.

Characteristics of clonally expanded thymocytes

To characterize clonally expanded thymocytes, we examined the cell cycle of the 95 40-day and 42 80-day thymocytes that were isolated from mice 1 h after injection of BrdU (Fig. 5A and B, Fig. E3). We defined the gated region on the FSC vs. SSC dot plot to exclude debris and dead cells. The percentage of the gated region markedly decreased, suggesting enhanced apoptosis. Figure 5B shows BrdU incorporation levels at the vertical axis and DNA contents at the horizontal axis. The DNA content of G1 cells did not differ among unirradiated, irradiated thymocytes, and lymphoma cells, which is consistent with the finding that even thymic lymphoma cells sustain diploidy (21). Figure 5C summarizes the percentage of S phase cells in T type and C type thymuses. Of the 40-day thymuses, no marked difference was found between T and C type thymuses. However, significant increase in the percentage was seen in C type thymus relative to T type thymus in the 80-day thymuses ($p = 0.0034$). Of note is that the high percentage of S cells is a hallmark of thymic lymphomas.

The size of G1 phase cells was measured with flow cytometry (Fig. 5B), because it represents the level of cell cycle progression and metabolic activity. The FSC values of G1 cells depicted a sharp peak in normal thymus, indicating a rather homogeneous cell-size population. The values were much smaller than those of S cells showing a broad peak, as predicted. The FSC analysis of 40-day and 80-day thymuses tended to show the values larger than normal thymus. The cell size of G1 cells in some atrophic thymuses exhibited a broad peak, indicating that those thymuses contained a fraction of larger-sized G1 cells more than normal thymuses did. We designated the cells in this fraction as middle-sized G1 cells because their size was between that of normal G1 and S phase cells. The middle-sized cells may be related to premalignancy because the cell-size enlargement was another characteristic of thymic lymphomas. The middle-sized G1 thymocytes are probably cells that are growing and progressing toward S phase but pausing at the late G1 stage.

Figure 5D summarizes the percentage of middle-sized G1 cells within the thymus. The percentage was determined in each thymus by the criterion whereby the percentage in normal thymus was set to approximately 5% in FSC analysis. The percentage showed a significant difference between T and C type thymuses in 40-day thymuses ($p = 0.014$), and the difference was more prominent in 80-day thymuses ($p = 0.0002$). Half of the 80-day C type thymuses exhibited the percentage more than 40%, whereas only 4 did so in the 21 T type thymuses. Notably, all thymic lymphomas consisted of middle-sized cells, suggesting that the C type middle-sized thymocytes are closer to lymphoma cells. Comparison between 40-day and 80-day thymuses suggests a process of irradiated thymuses toward thymic lymphoma in the order of T type thymus, C type thymus with a low percentage of middle-G1 cells, and C type thymus with a high percentage of middle-G1 cells.

Figure 5E summarizes the percentage of middle-sized G1 cells in *Bcl11b* allelic loss-negative and -positive thymuses. The two groups of 40-day thymuses showed difference in the percentage ($p = 0.041$). The 80-day thymocytes also showed a difference between the two ($p = 0.017$). This suggests the contribution of *Bcl11b*-allelic loss to cell cycle progression. On the other hand, no significant difference in the percentage of S cells was observed between the two groups (not shown).

No marked change in DNA damage checkpoint response

Deoxyribonucleic acid damage checkpoints are activated in premalignant cells and thought to act as barriers against